GA17-06

Results from CALorimetric Electron Telescope (CALET) Observations of Gamma-rays on the International Space Station

Masaki Mori

Ritsumeikan University

Nicholas Cannady

University of Maryland and NASA/GSFC

for the CALET collaboration

ICRC2023, Nagoya, Japan, July 26-August 3, 2023

The CALET collaboration

O. Adriani[1,2], Y. Akaike[3,4], K. Asano[5], Y. Asaoka[5], E. Berti[2,6], G. Bigongiari[7,8], W.R. Binns[9], S. Bonechi[29], M. Bongi[1,2], P. Brogi[7,8], A. Bruno[10], N. Cannady[11,12,13], G. Castellini[6], C. Checchia[7,8],M.L. Cherry[14], G. Collazuol[15,16], G.A. de Nolfo[10], K. Ebisawa[17], A.W. Ficklin[14], H. Fuke[17], S. Gonzi[1,2,6], T.G. Guzik[14], T. Hams[11], K. Hibino[18], M. Ichimura[19], K. Ioka[20], W. Ishizaki[5], M.H. Israel[9], K. Kasahara[21], J. Kataoka[22], R. Kataoka[23], Y. Katayose[24], C. Kato[25], N. Kawanaka[20], Y. Kawakubo[14], K. Kobayashi[3,4], K. Kohri[26], H.S. Krawczynski[9], J.F. Krizmanic[12], P. Maestro[7,8], P.S. Marrocchesi[7,8], A.M. Messineo[8,27], J.W. Mitchell[12], S. Miyake[28], A.A. Moiseev[29,12,13], M. Mori[30], N. Mori[2], H.M. Motz[18], K. Munakata[25], S. Nakahira[17], J. Nishimura[17], S. Okuno[18],J.F. Ormes[31], S. Ozawa[32], L. Pacini[2,6], P. Papini[2], B.F. Rauch[9], S.B. Ricciarini[2,6], K. Sakai[11,12,13], T. Sakamoto[33], M. Sasaki[29,12,13], Y. Shimizu[18], A. Shiomi[34], P. Spillantini[1], F. Stolzi[7,8], S. Sugita[33], A. Sulaj[7,8], M. Takita[5], T. Tamura[18], T. Terasawa[5], S. Torii[3], Y. Tsunesada[35,36], Y. Uchihori[37], E. Vannuccini[2], J.P. Wefel[14], B. K. Yamaoka[38], S. Yanagita[39], A. Yoshida[34], K. Yoshida[21] , and W.V. Zober[9]

1) University of Florence, Italy
2) INFN Sezione di Florence, Italy
3) RISE, Waseda University, Japan
4) JEM Utilization Center, JAXA, Japan
5) ICRR, University of Tokyo, Japan
6) IFAC (CNR) and INFN, Italy
7) University of Siena, Italy
8) INFN Sezione di Pisa, Italy
9) Washington University-St. Louis, USA
10) Heliospheric Phys. Lab., NASA/GSFC, USA
11) CSST, University of Maryland, USA
12) Astroparticle Phys. Lab., NASA/GSFC, USA
13) CRESST, NASA/GSFC, USA
14) Louisiana State University, USA
15) University of Padova, Italy
16) INFN Sezione di Padoa, Italy
17) ISAS, JAXA, Japan
18) Kanagawa University, Japan
19) Hirosaki University, Japan
20) YITP, Kyoto University, Japan
21) Shibaura Institute of Technology, Japan
22) SASE, Waseda Universtiy, Japan
23) National Inst. For Polar Research, Japan
24) Yokohama National University, Japan
25) Shinshu University, Japan
26) INS, KEK, Italy
27) University of Pisa, Italy
28) National Inst. of Technology (KOSEN), Japan
29) University of Maryland, USA
30) Ritsumeikan University, Japan
31) University of Denver, USA
32) National Inst. Of Information and Comm. Tech., Japan
33) Aoyama Gakuin University, Japan
34) Nihon University, Japan
35) Osaka Metropolitan University, Japan
36) NYITEP, Osaka Metropolitan University, Japan
37) National Inst. For Quantum and Rad. Sci. Tech., Japan
38) Nagoya University, Japan
39) Ibaraki University, Japan

See Highlight talk by Torii (2-01) for the summary of CALET results!

CALET Payload

Kounotori (HTV) 5

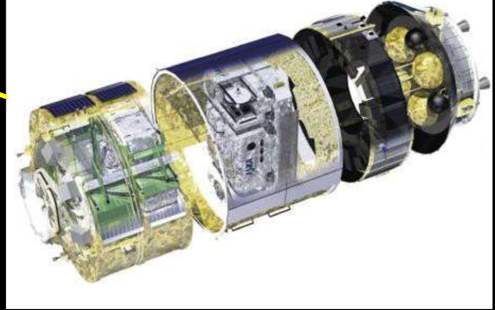

Launched on Aug. 19th, 2015 by the Japanese H2-B rocket

Emplaced on JEM-EF port #9 on Aug. 25th, 2015 (JEM-EF: Japanese Experiment Module-Exposed Facility)

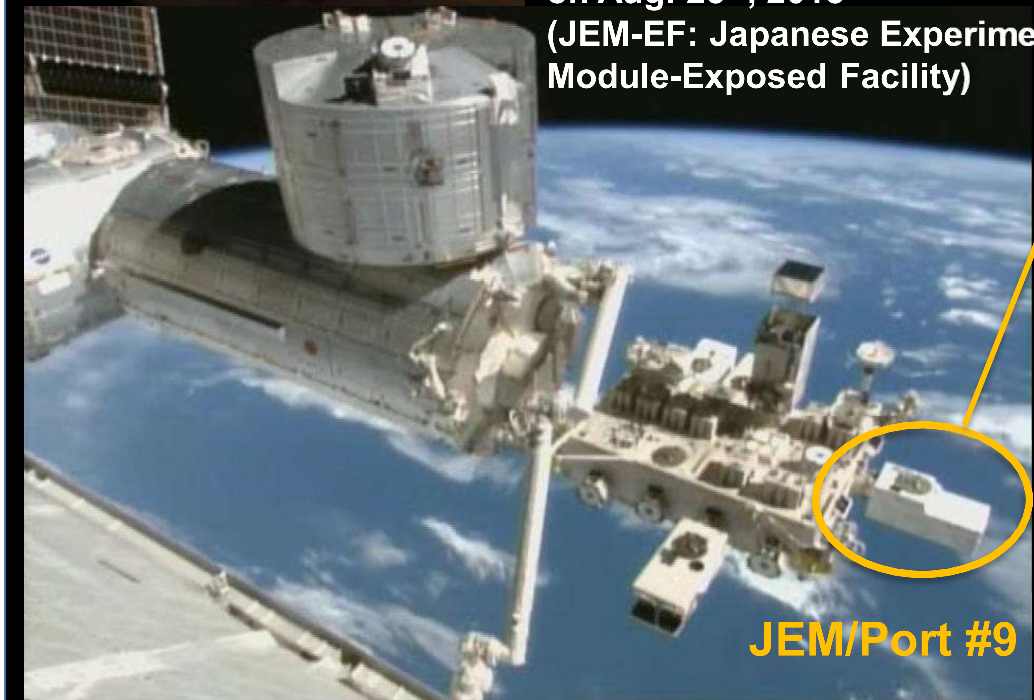

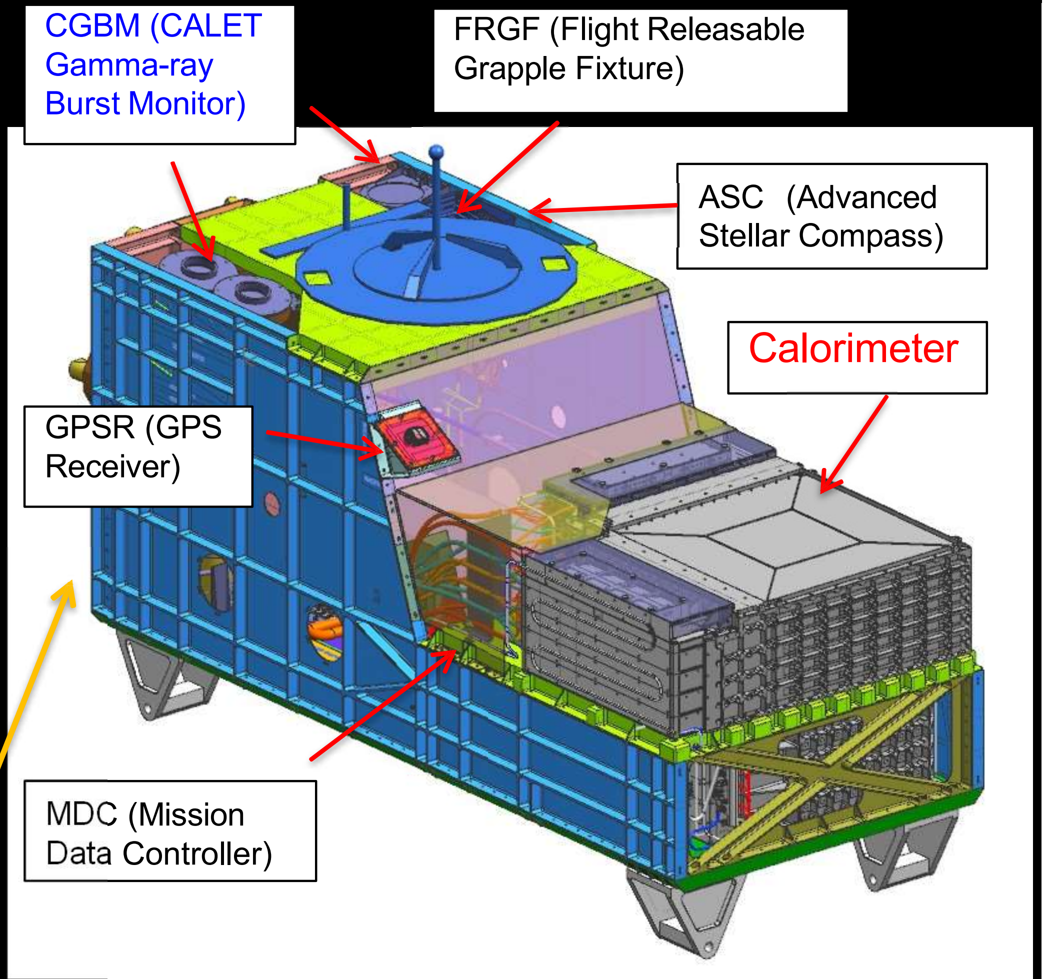

- **Mass: 612.8 kg**
- **JEM Standard Payload Size: 1850mm(L) × 800mm(W) × 1000mm(H)**
- **Power Consumption: 507 W（max）**
- **Telemetry: Medium 600 kbps (6.5GB/day) / Low 50 kbps**

CALET/CAL schematics

Fully active thick calorimeter ($30X_0$) optimized for electron spectrum measurements well into TeV region

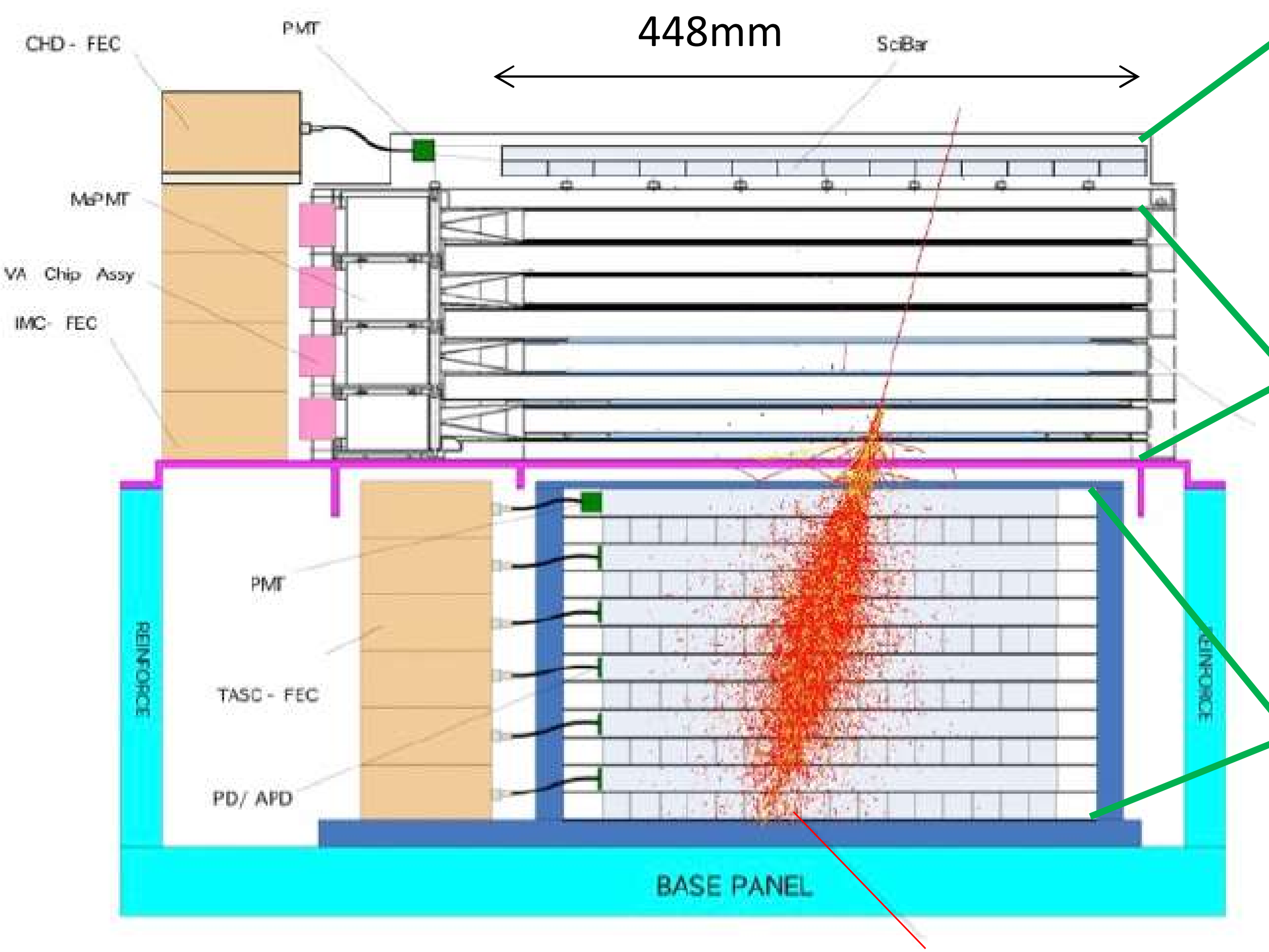

1TeV electron shower is fully contained in TASC

Charge Detector **CHD**

plastic scintillator hodoscope,
absolute charge measurement
(including charge zero)

Imaging Calorimeter **IMC**

SciFi + tungsten plate ($3X_0$),
reconstruction of arrival direction and initial shower development

Total Absorption Calorimeter **TASC**

PWO hodoscope ($27X_0$),
energy measurements and particle identification

Gamma Ray Event Selection

Cannady et al., ApJS 238:5 (2018)

= Electron Selection Cut + Gamma-ray ID Cut w/ Lower Energy Extension

<u>100 GeV Event Examples</u>

gamma-ray	electron	proton
Charge Z=0	Charge Z=1	

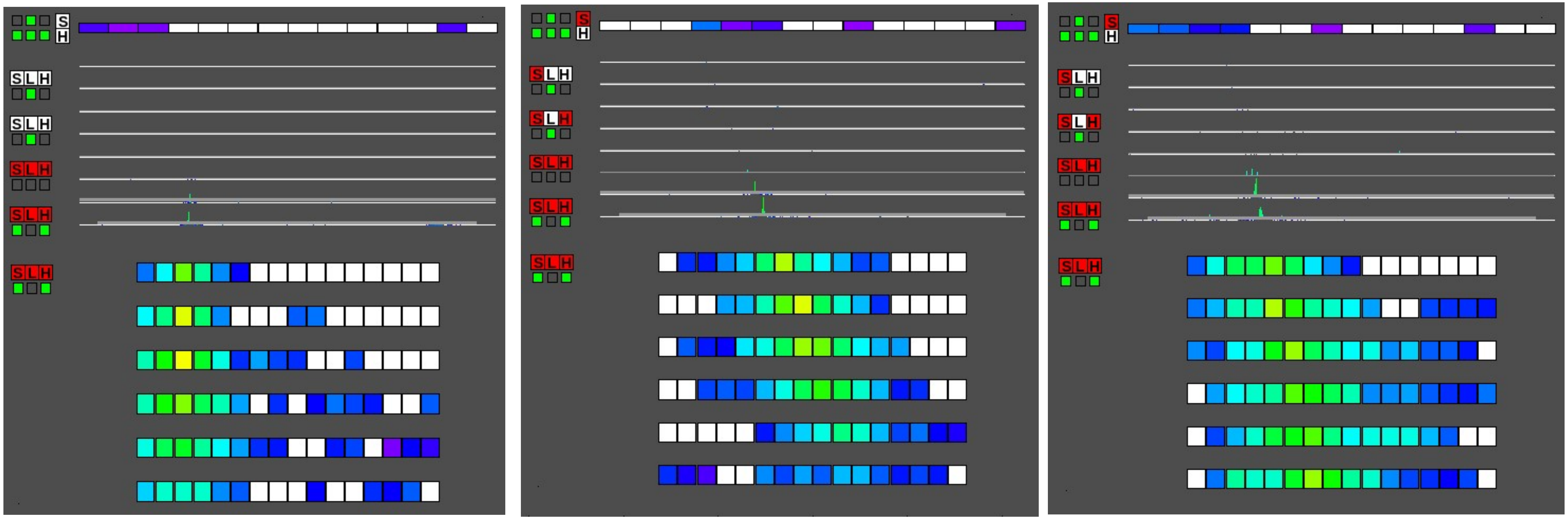

Electromagnetic Shower		Hadron Shower
well contained, constant shower development		larger spread

CALET triggers and gamma-ray observation

Trigger rate vs ISS location

Asaoka et al., Astropart.Phys. 100, 29 (2018)

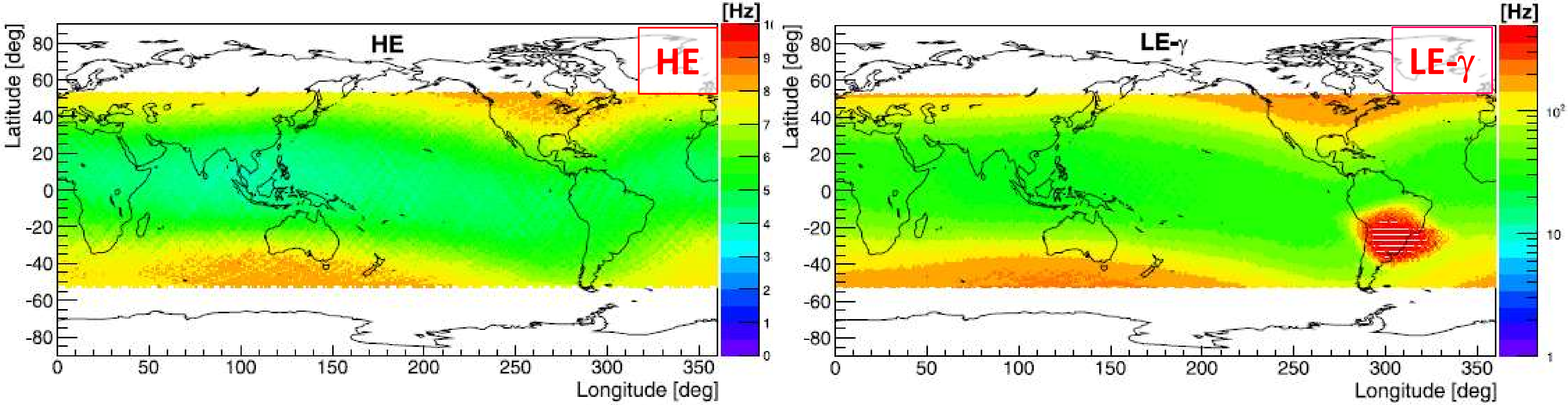

Typical operation

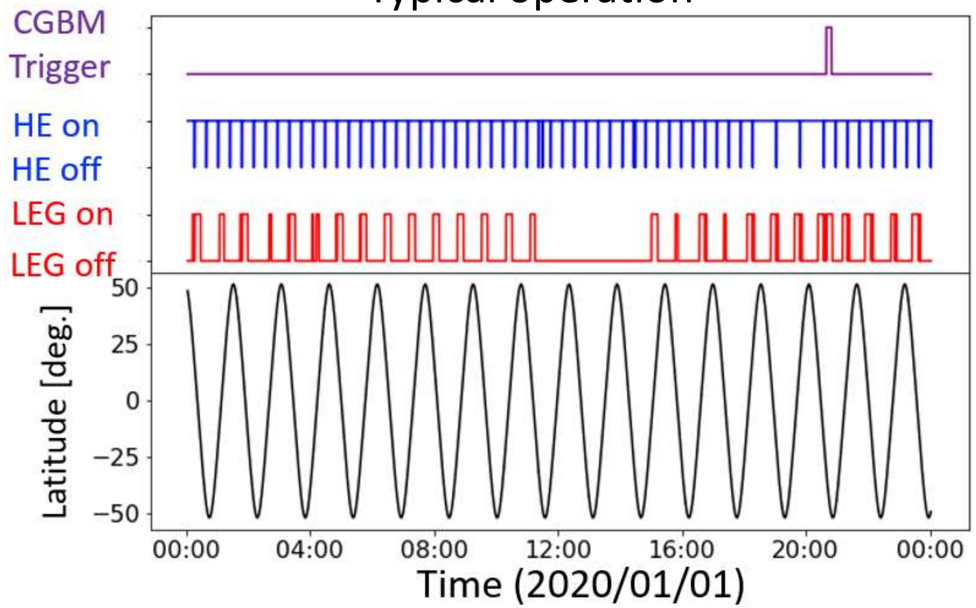

HE trigger: $E_\gamma > 10$ GeV
LE-γ trigger: $E_\gamma > 1$ GeV

- HE trigger mode: always ON
- LE-γ mode: ON when geomag.lat. < 20° or CALET Gamma-ray Burst Monitor (CGBM) is triggered

Gamma Ray Event Selection in CAL

= Electron Selection Cut + Gamma-ray ID Cut w/ Lower Energy Extension

It was found that secondary gamma rays produced in ISS structures are dominant source of background

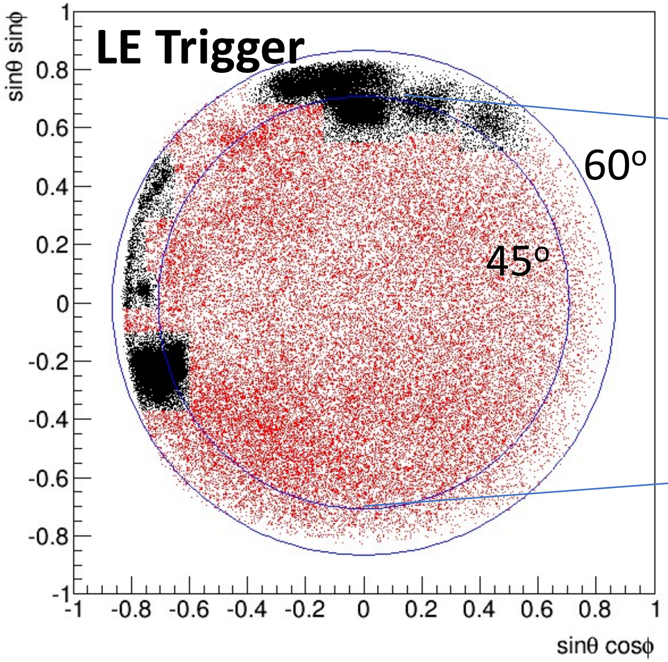

Gamma-ray candidates in CALET FOV

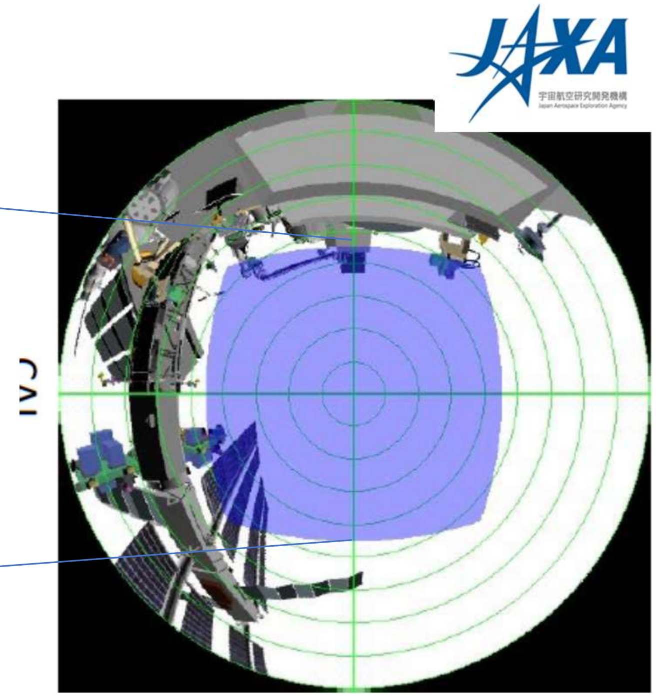

Fish-eye view of CALET FOV

By removing Black parts, it is possible to reject majority of such background. More sophisticated rejection method has been developed (see next slide).

1. Geometry Condition
   - CHD-Top to TASC 1st layer (2cm margin)
2. Preselection
   - Offline trigger
   - Shower concentration
   - Shower starting point
3. Track quality cut
   - Track hits >2
   - matching w/ TASC
4. Electromagnetic shower selection
   - shower shape
5. Gamma-ray ID
   - CHD-veto
6. FOV cut

Improved Gamma Ray Event Selection

Cannady et al., PoS (ICRC2021)

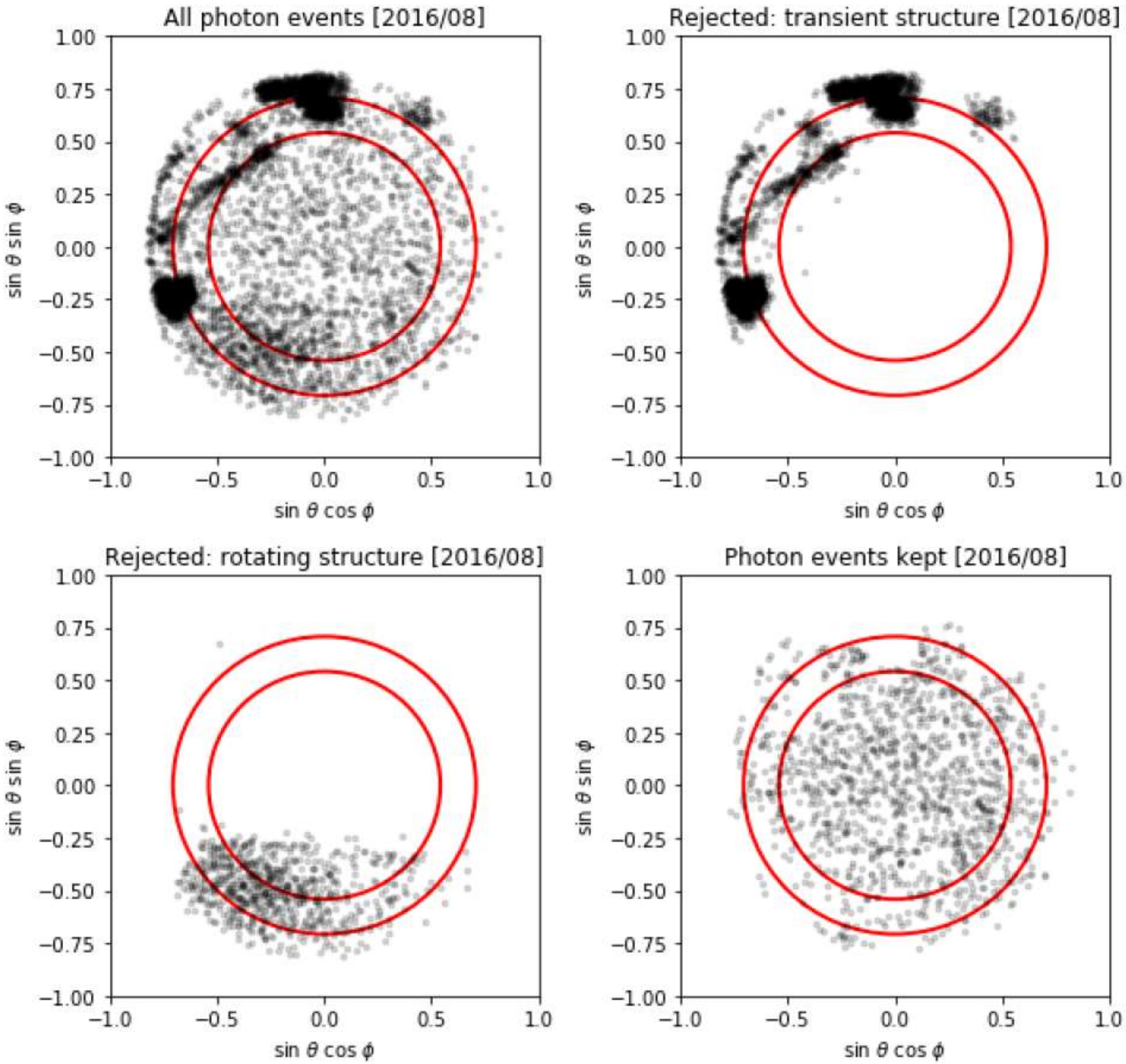

One month of gamma-ray candidates with various obstructions. Clockwise from upper left: all candidates; candidates removed by manually defined cuts; candidates removed as coming from rotating structures; events kept after FOV cuts. (Red circles: 45° and 60° from zenith.)

Monthly maps and daily maps are checked to keep our field-of-view clear.

See poster by N. Cannady (PCRD3-07) for discussion on environment of detectors on ISS!

CALET performance

- **HE** trigger (>10 GeV) is always active in normal observations
- **LE-γ** trigger (>1 GeV) mode is activated when the geomagnetic latitude is below 20° or following a CALET Gamma-ray Burst Monitor (CGBM) burst trigger

Angular resolution

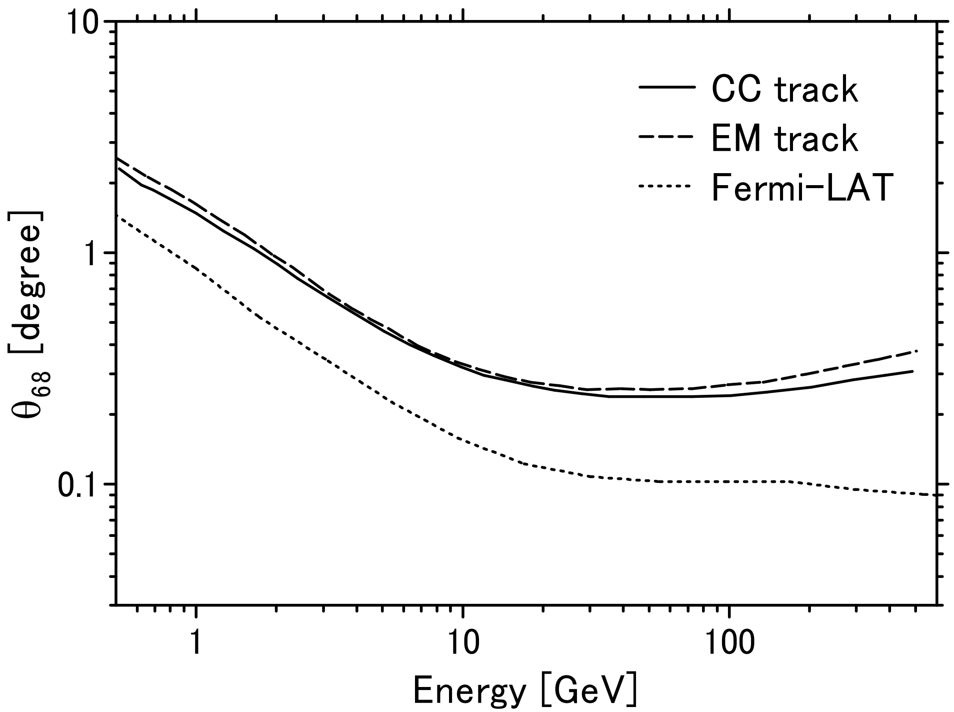

Cannady et al., ApJS 238, 5 (2018)

Energy resolution

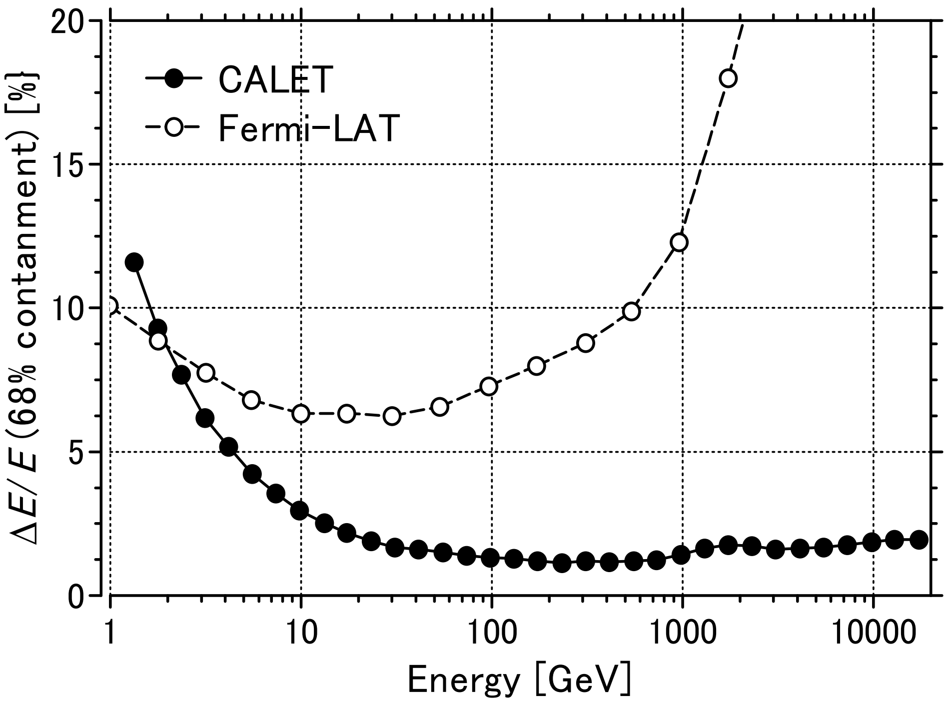

Asaoka et al, Astropart. Phys. 91, 1 (2017)

- Good energy resolution at high energies thanks to the thick calorimeter!

Gamma-ray skymaps

Preliminary

November 2015 – December 2022

LE-γ trigger (>1 GeV)

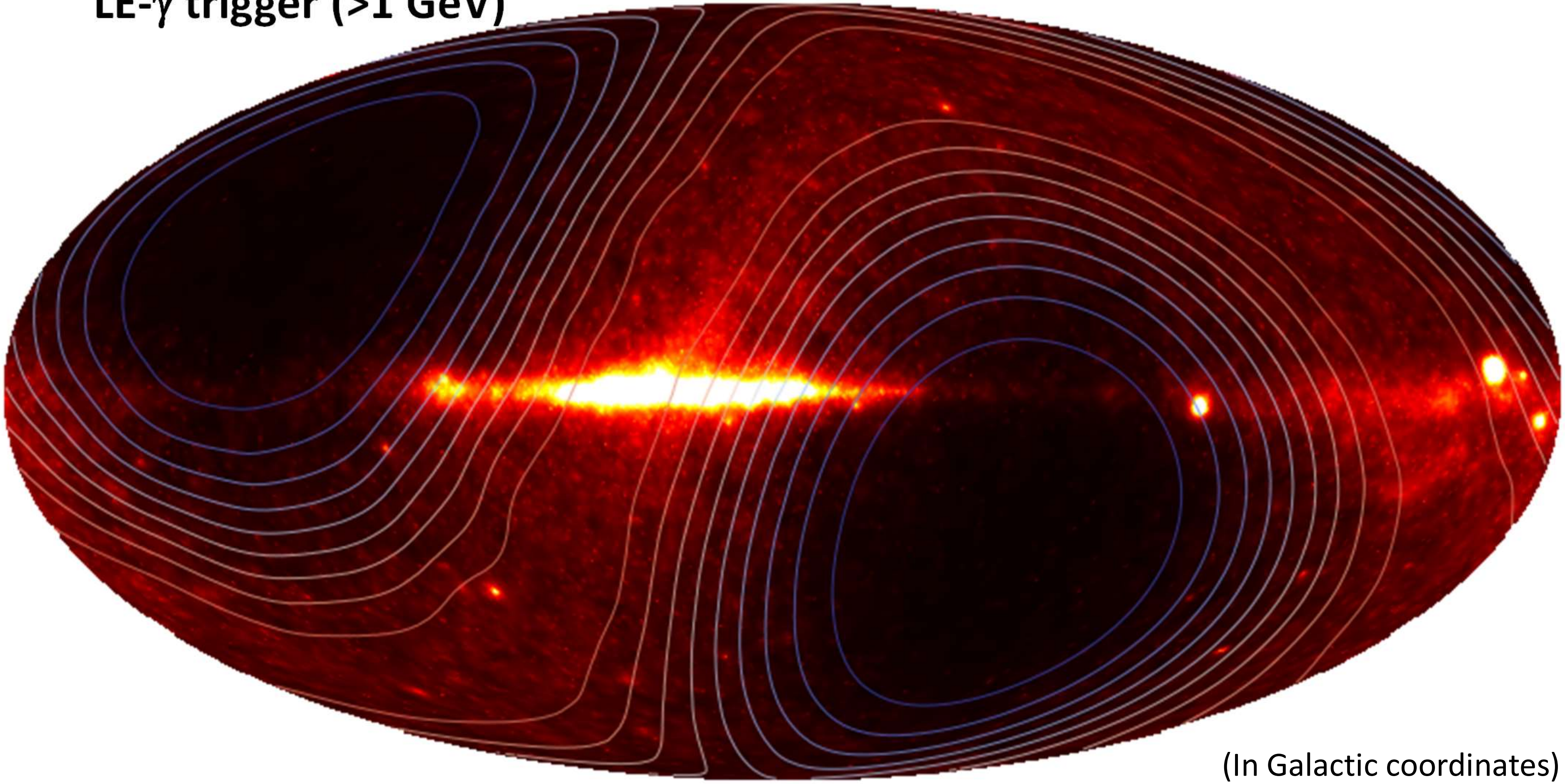

(In Galactic coordinates)

Note: Exposure (shown by contours) is not uniform due to the ISS orbit (inclination 51.6°)

Gamma-ray skymaps

Preliminary

November 2015 – December 2022

HE trigger (>10 GeV)

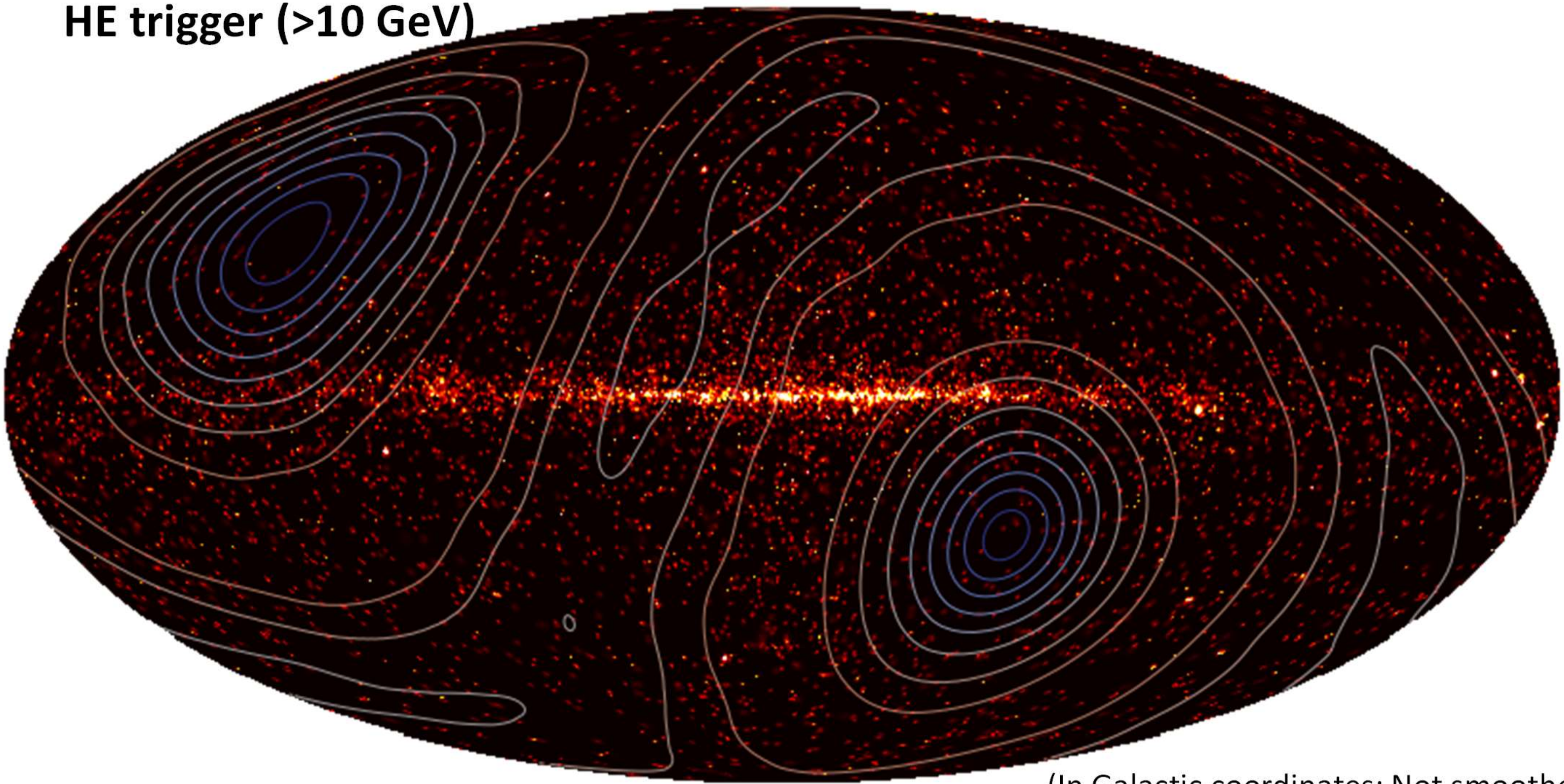

(In Galactic coordinates; Not smoothed)

Note: Exposure (shown by contours) is not uniform due to the ISS orbit (inclination 51.6°)

Energy spectra for bright point sources

Preliminary

November 2015 – December 2022

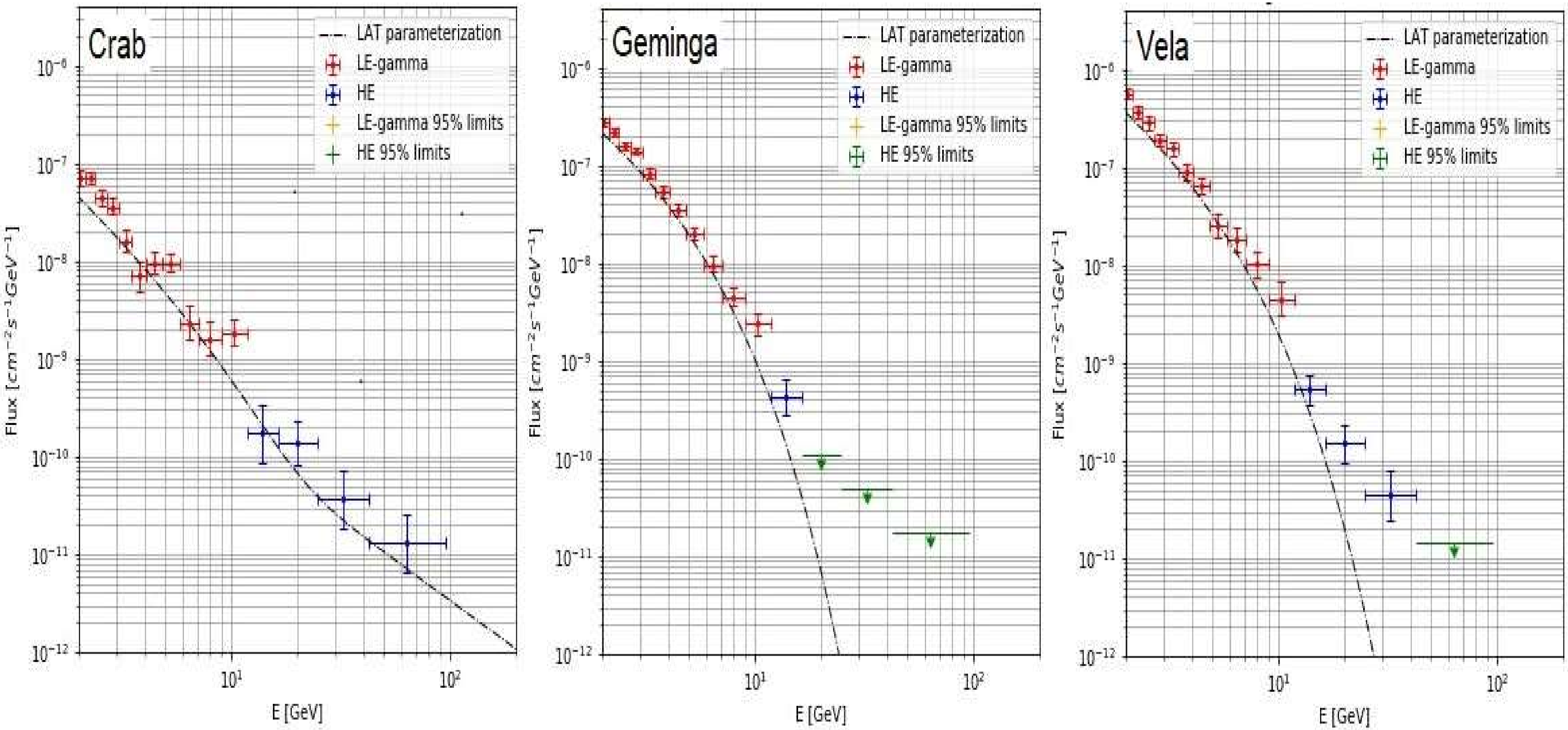

- Consistent with Fermi-LAT spectra

AGN light curves

Preliminary

November 2015 – December 2022

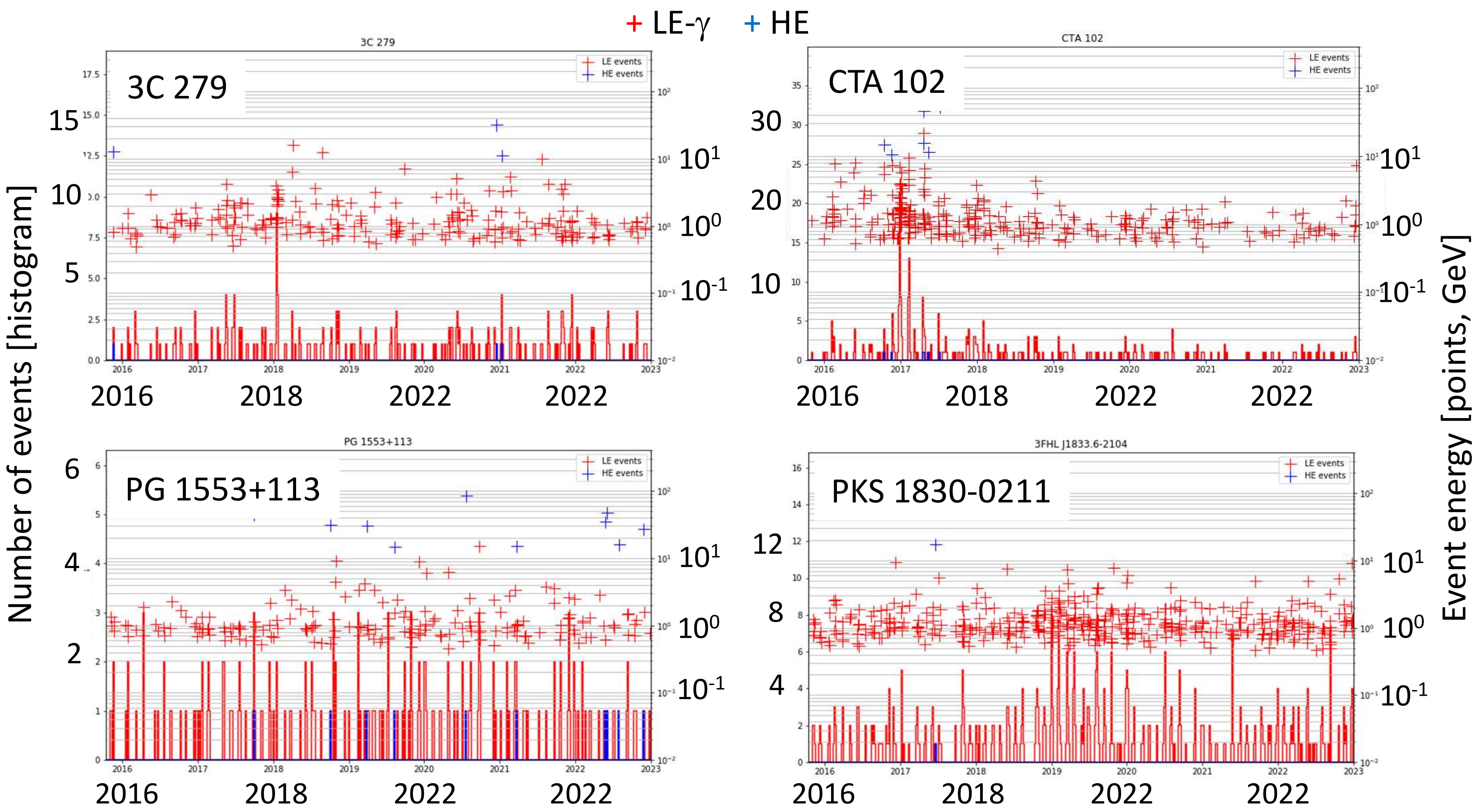

- Working as a long-range monitor

Gamma-ray spectra (LE-γ & HE)

Preliminary

November 2015 – December 2022

(Fermi data: analyzed from public data.)

LE-γ trigger **HE trigger**

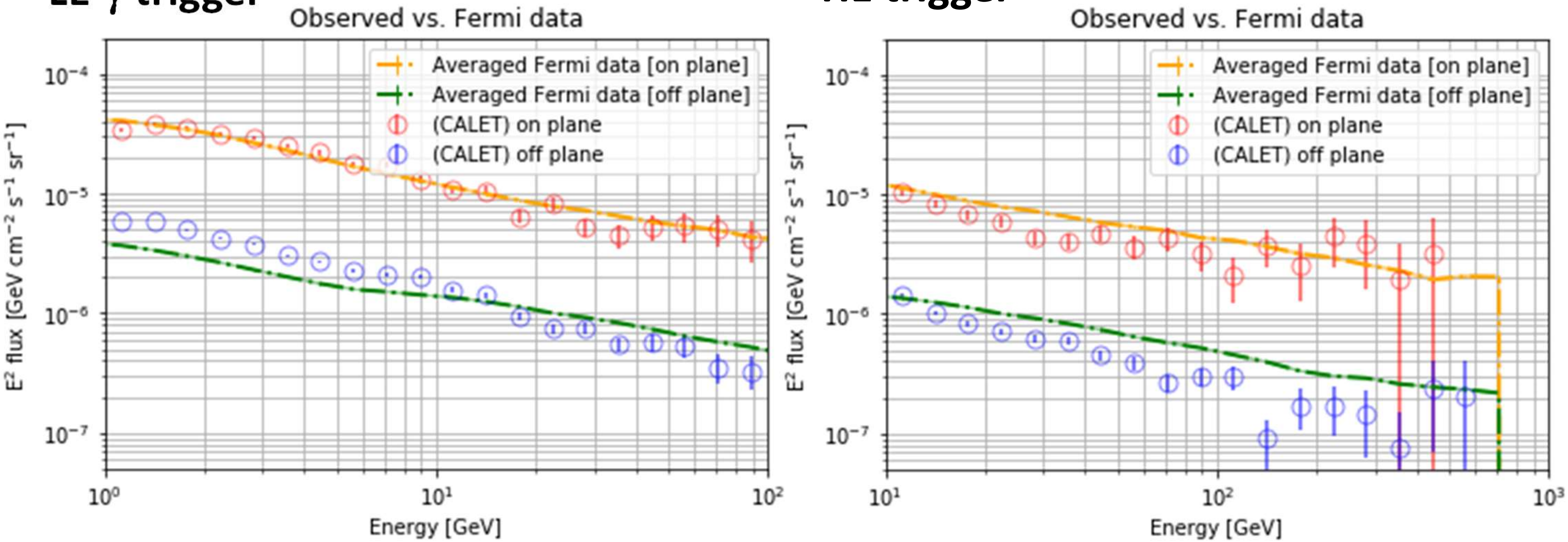

"**On-plane**": $|l| < 80°$ & $|b| < 8°$, "**Off-plane**": $|b| > 10°$

- The spectra (Galactic diffuse + point sources) look fairly consistent with those by Fermi-LAT.

Improvements to HE sensitivity

- At higher energies, charge selection with CHD becomes contaminated with backscattered secondary particles.

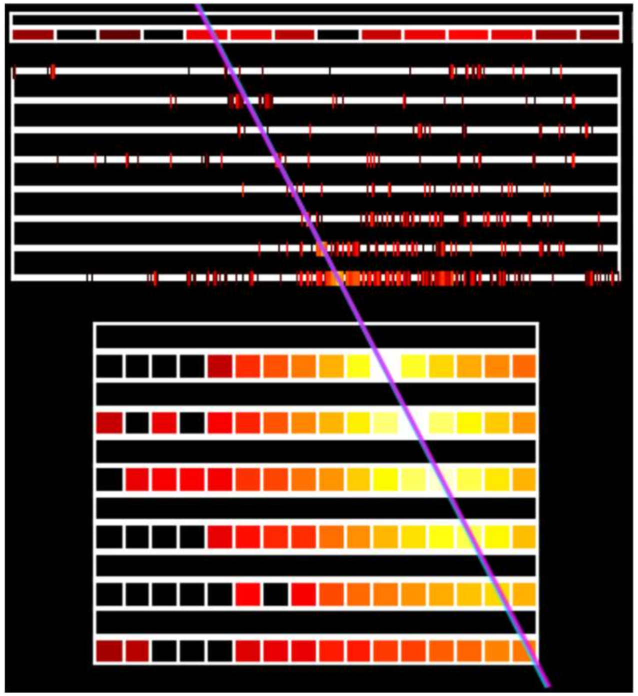

- New selection defined to use looser cuts in CHD and incorporating first two layers of IMC for charged primary rejection
- Preliminary results show significant increase in effective area $E > 100$ GeV
- Testing of selection and contamination being finalized for implementation in all analyses soon!

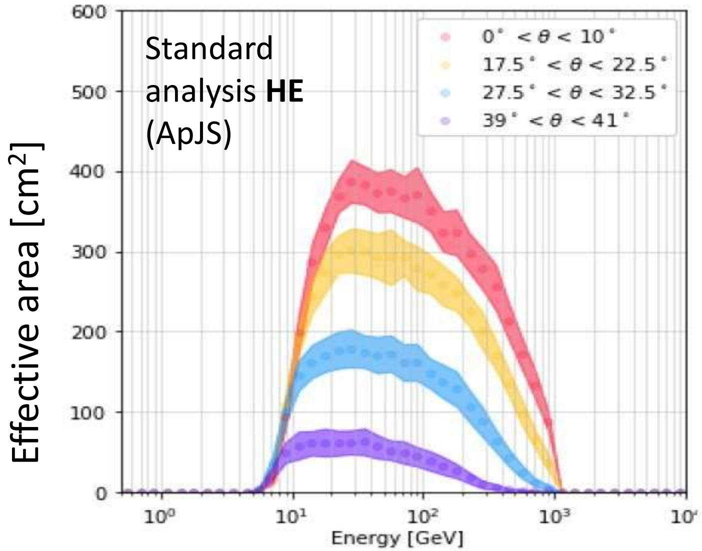

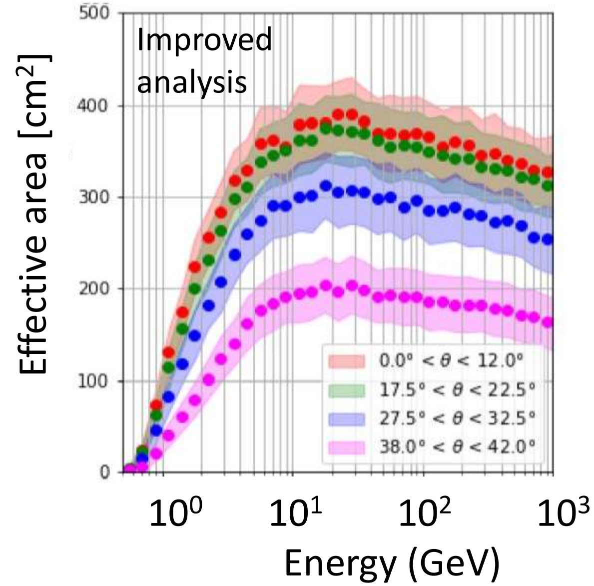

See poster (Cannady et al., PGA2-10) for details.

Summary

- CALET has been observing celestial gamma ray above 1 GeV for more than 7.5 years since its launch in October 2015.
- Point sources and diffuse gamma-rays are studied, and they are consistent with Fermi-LAT results.
- Improvements to high-energy (>100 GeV) sensitivities are going on…
  - Present analysis is optimized for the GeV energy range.
  - Significant increase in effective area is expected in the 100 GeV region with the new analysis under development if applied to Monte Carlo data.
  - Next, we try to apply the new analysis to flight data.

Backups

Fermi-LAT light curves

3C 279

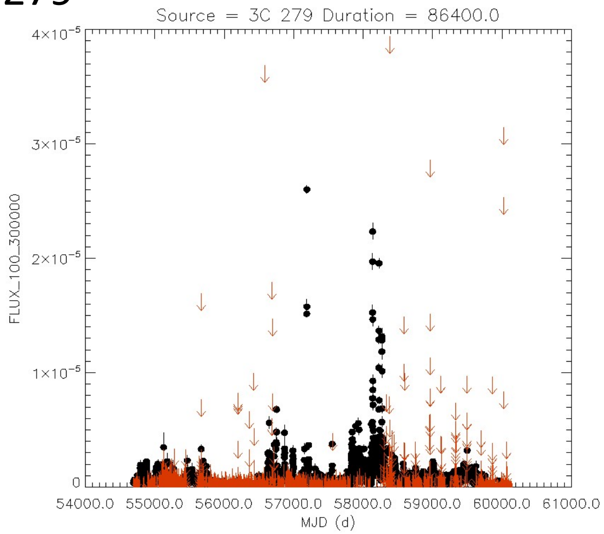

CTA 102

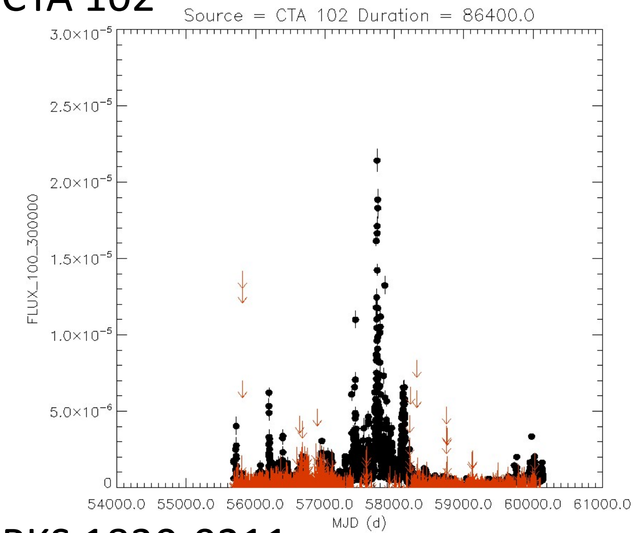

PG 1553+113

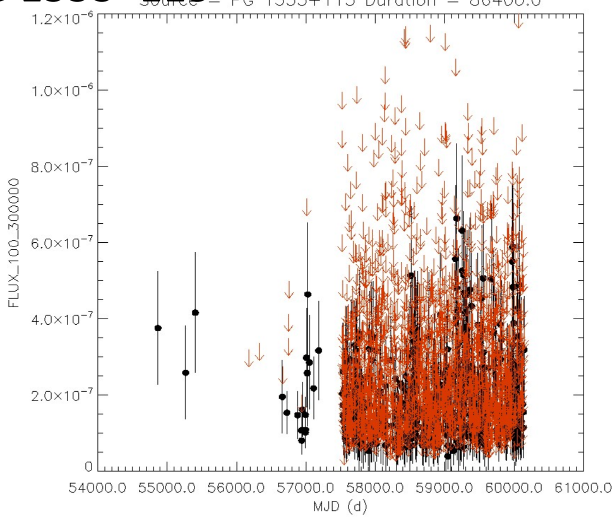

PKS 1830-0211

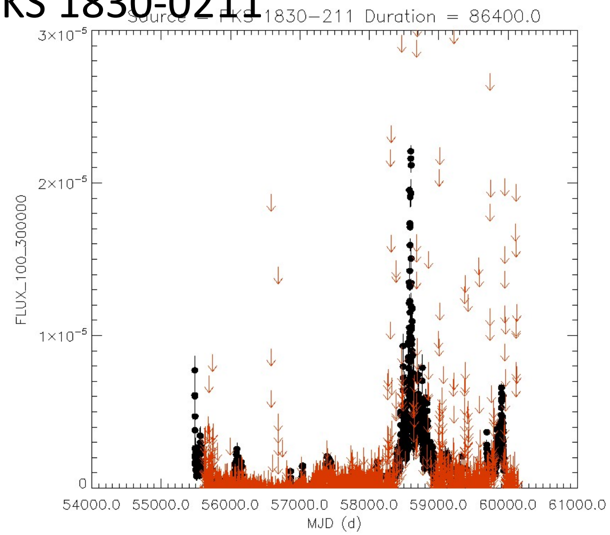

MJD 58000 =
Sep 04, 2017

MJD 59000 =
May 31, 2020

MJD 60000 =
Feb 25, 2023

Transient follow-ups

- Trigger of CGBM instrument prompts CALET to temporarily activate LE-γ mode to search for transient counterparts
- Transient analysis pipeline allows for quick follow-up of GRBs or LIGO/Virgo GW triggers
- Observations corresponding to triggers in LIGO/Virgo O3 run recently published in **Adriani et al., ApJ 933 85 (2022)**.
- Waiting for O4 to start…

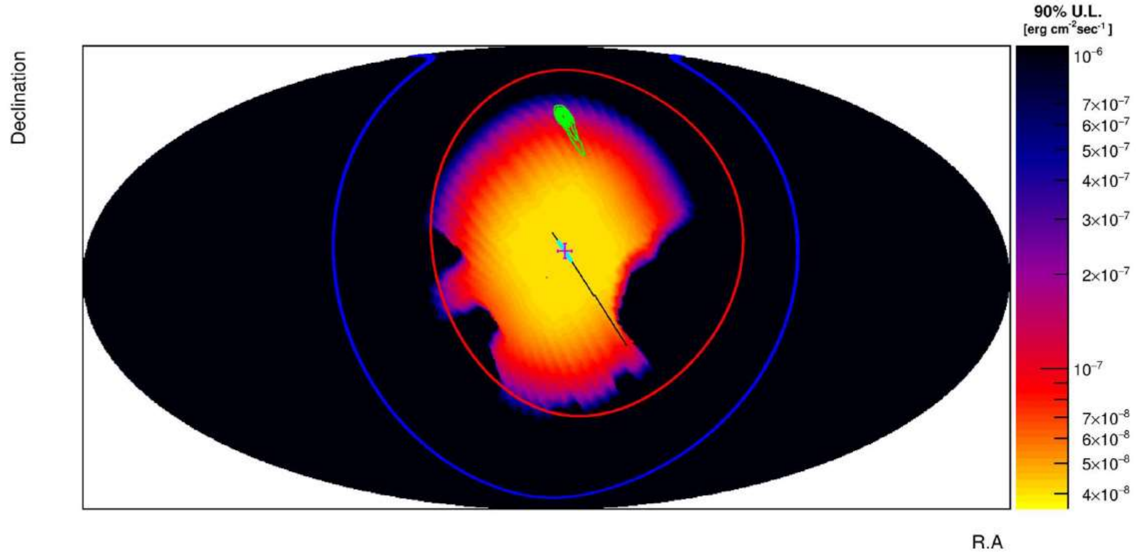

Figure 10. 90% confidence level upper limits observed by CAL in the energy range 1–10 GeV during the interval ±60 s around the time of GW190408an reported by LIGO/Virgo. The intensity scale is given in units of erg cm^{-2} s^{-1}. Red and blue circles are the HXM and SGM fields of view, respectively.

Fermi-LAT

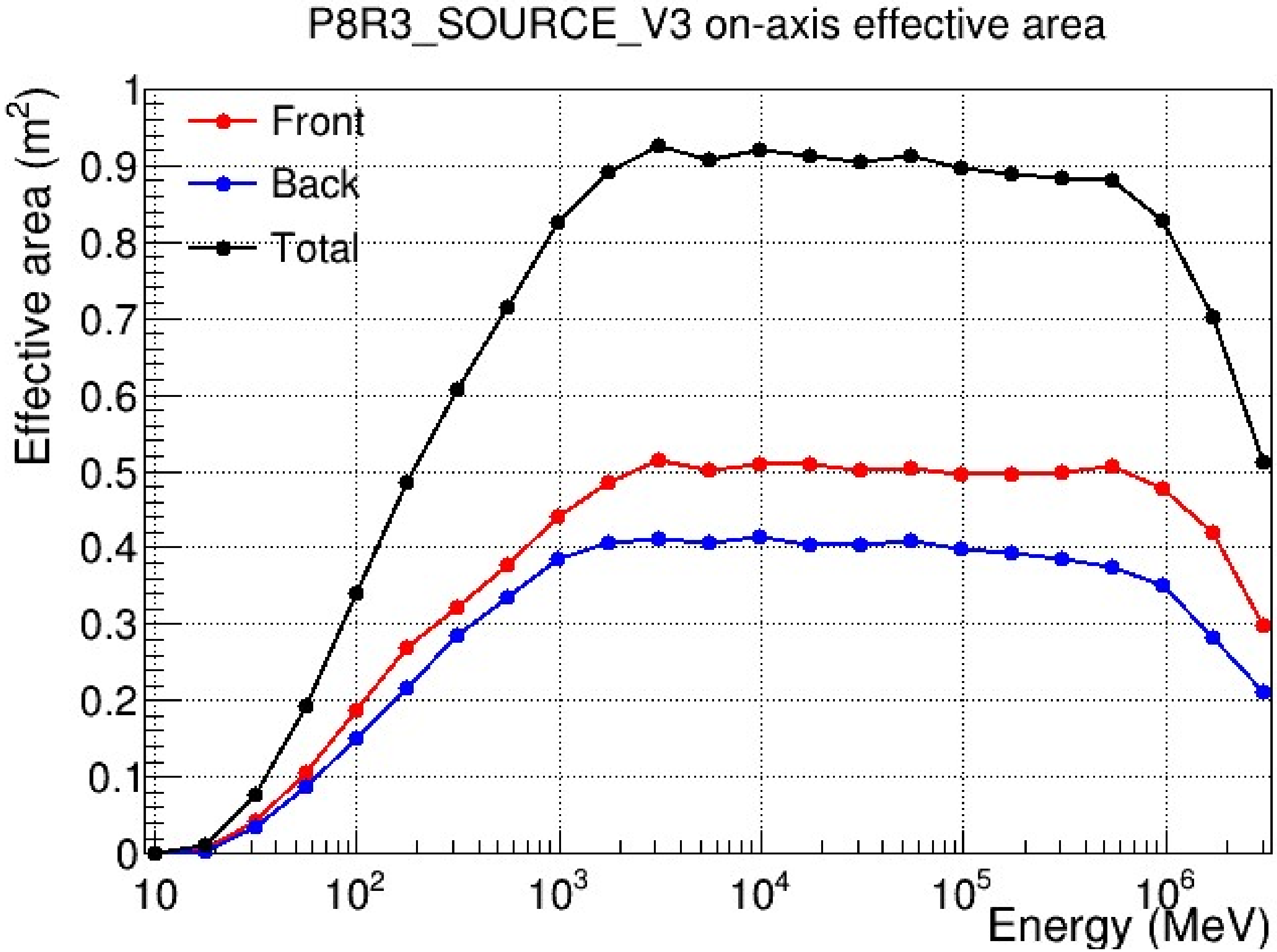

https://www.slac.stanford.edu/exp/glast/groups/canda/lat_Performance.htm

Point spread function (PSF)

$$P(\theta_s) = f_{core}K(\theta_s, \sigma_{core}, \gamma_{core}) + (1 - f_{core})K(\theta_s, \sigma_{tail}, \gamma_{tail}) \qquad K(\theta_s, \sigma, \gamma) = \frac{1}{2\pi\sigma^2}\left(1 - \frac{1}{\gamma}\right)\left[1 + \frac{1}{2\gamma}\frac{\theta_s^2}{\sigma^2}\right]^{-\gamma}$$

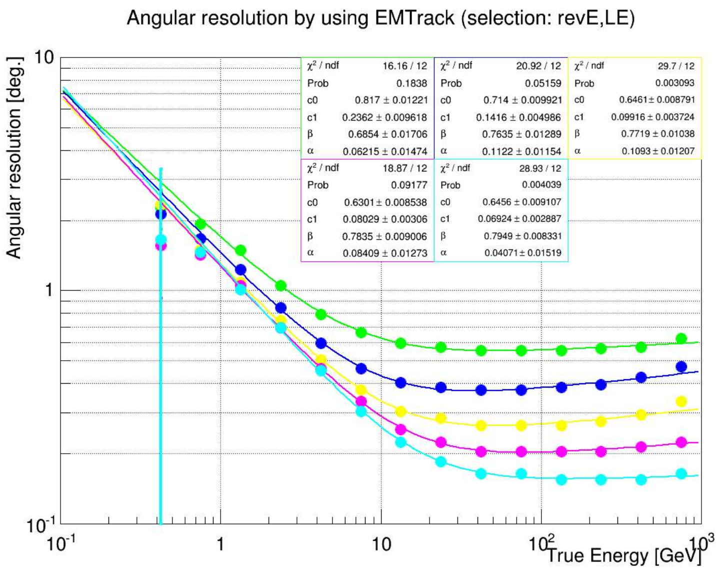

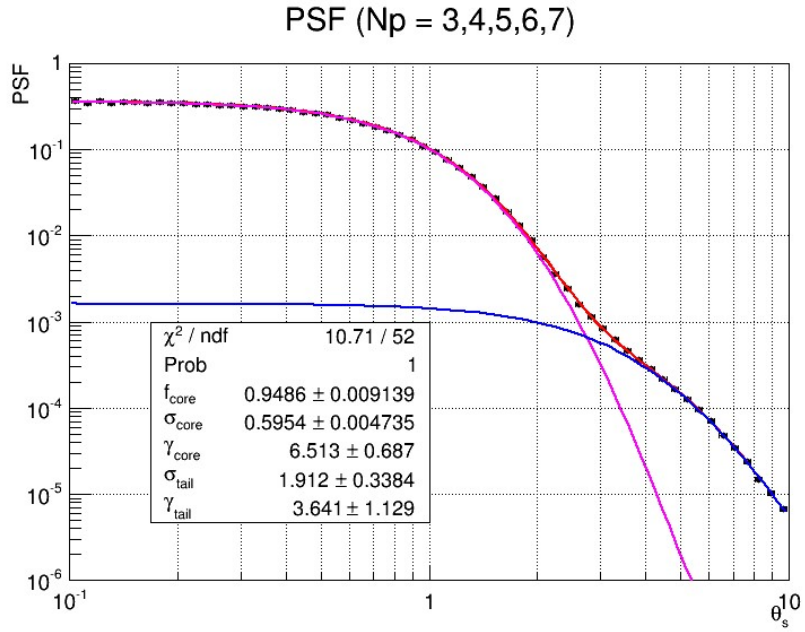

N_p : number of track points used for reconstruction

Np=3 Np=4 Np=5

Np=6 Np=7

—core

—tail

—core + tail

Original (ApJS) definition of geometry E

Acceptance	Conditions			Geom. Fact. $[cm^2 sr]$
A	CHD top	TASC top*	TASC 6y bottom*	419.1
EB	CHD top	TASC top*	TASC 6y bottom	91.03
ED	CHD top	TASC top*	TASC path > 24 cm	121.6
EB3	CHD top	TASC top*	TASC 3y bottom*	51.97
ED3	CHD top	TASC top*	TASC 3y bottom	127.9
E	CHD top	TASC top*		373.8

Table 3.1: Requirements for the LE-γ geometrical conditions. The conditions marked with asterisks denote that the intersection point must be more than 2 cm from the edge of the layer boundary.

LE-γ analysis uses A–E: total 1185.4 cm^2sr
HE analysis uses A–ED: total 631.73 cm^2sr

Compare to standard acceptance:

	Condition	SΩ[cm2sr]
A	CHD-X-top && CHD-Y-top && TASC-top (inside 1 log) && TASC-bot (inside 1 log)	A: 415.7 ± 1.1
B	CHD-X-top && CHD-Y-top && TASC-top && TASC-bot && ! { TASC-top (inside 1log) && TASC-bot (inside 1log) }	B: 154.6±0.7 A+B: 570.3±1.3
C	IMC5th layer && TASC-top && TASC-bot && ! { CHD-X-top && CHD-Y-top }	C: 230.1±0.8 A+B+C: 800.4±1.6
D	IMC5th layer && TASC-top && path length in TASC > thickness of TASC && !TASC-bot	D: 236.4±0.8 A+B+C+D:1036.6±1.8

Revised definition of geometry E

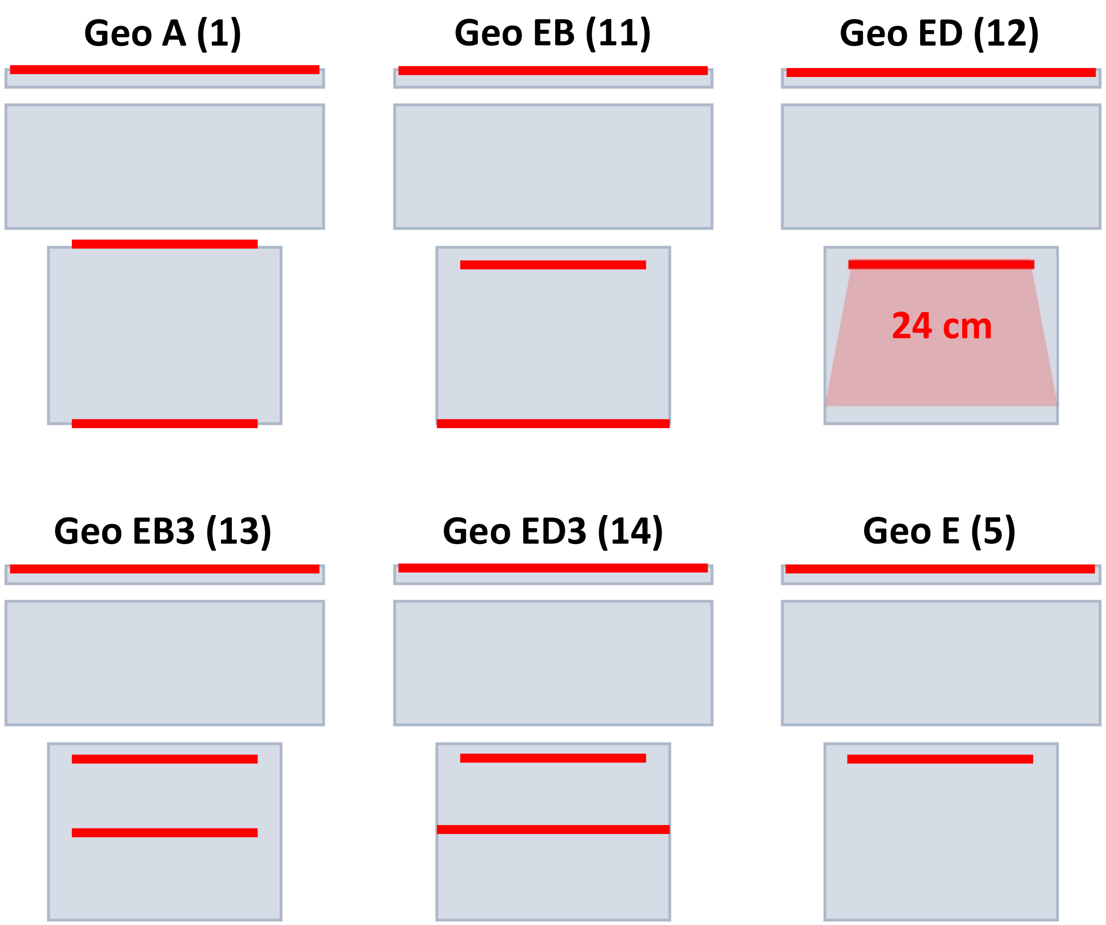

Acceptance	Conditions			Geom. Fact. $[cm^2 sr]$ (exclusive)	(cumulative)
A	CHD top	TASC top*	TASC 6y bottom*	419.11	419.11
EB	CHD top	TASC top*	TASC 6y bottom	91.03	510.14
ED	CHD top	TASC top*	TASC path > 24 cm	121.55	631.69
EB3	CHD top	TASC top*	TASC 3y bottom*	51.97	683.65
ED3	CHD top	TASC top*	TASC 3y bottom	127.94	811.59
E	CHD top	TASC top*		372.81	1184.4

Table 3.1: Requirements for the LE-γ geometrical conditions. The conditions marked with asterisks denote that the intersection point must be more than 2 cm from the edge of the layer boundary.

Should have been bottom of TASC X1 rather than top for better containment

Better energy resolution for only small change in geometrical factor:

Acceptance	Conditions			Geom. Fact. $[cm^2 sr]$ (exclusive)	(cumulative)
A	CHD top	TASC top*	TASC 6y bottom*	419.11	419.11
EB	CHD top	TASC X1 bot*	TASC 6y bottom	99.20	518.31
ED	CHD top	TASC X1 bot*	TASC path > 24 cm	122.16	640.57
EB3	CHD top	TASC X1 bot*	TASC 3y bottom*	53.26	693.72
ED3	CHD top	TASC X1 bot*	TASC 3y bottom	125.78	819.51
E	CHD top	TASC X1 bot*		277.17	1096.68

Table 3.1: Requirements for the LE-γ geometrical conditions. The conditions marked with asterisks denote that the intersection point must be more than 2 cm from the edge of the layer boundary.